



# Macroporous–mesoporous alumina supported iridium catalyst for hydrazine decomposition

Ik Jun Jang<sup>a</sup>, Hye Sun Shin<sup>a</sup>, Na Ra Shin<sup>a</sup>, Su Hyun Kim<sup>a</sup>, Su Kyum Kim<sup>b,\*\*</sup>, Myoung Jong Yu<sup>b</sup>, Sung June Cho<sup>a,\*</sup>

<sup>a</sup> Clean Energy Technology Laboratory and Department of Applied Chemical Engineering, Chonnam National University, Gwangju 500-757, Republic of Korea

<sup>b</sup> Satellite Thermal and Propulsion Department, Korea Aerospace Research Institute, Daejeon 305-333, Republic of Korea

## ARTICLE INFO

### Article history:

Available online 29 September 2011

### Keywords:

Hydrazine decomposition

Satellite

Ir nanoparticles

ρ-Alumina

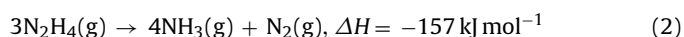
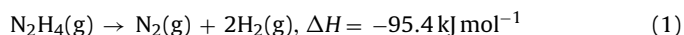
## ABSTRACT

Decomposition of hydrazine allows the attitude and altitude control of satellite. Macroporous–mesoporous alumina supported iridium catalyst (KCMC-7) has been developed using the fast dehydration of aluminium trihydroxide and subsequent multiple impregnations. The result of data analysis suggested that the obtained alumina was ρ-Al<sub>2</sub>O<sub>3</sub> with both macro and mesopores. Significant amount of pentagonal Al sites after rehydration of ρ-Al<sub>2</sub>O<sub>3</sub> was responsible for ultra high dispersion for ultra high loading of metal around 30 wt%. The performance of the KCMC-7 measured using 4.5 N dual thruster module was satisfactory until the end of life, providing enough thrust for the attitude and altitude control of satellite in the pressure range of 50–350 psi.

© 2011 Elsevier B.V. All rights reserved.

## 1. Introduction

Telecommunication mediated by satellites is now essential part of human life. Numerous satellites orbit around the Earth to transmit signal one region to another. It is known that the life of satellite is determined by the amount of fuel and the life of catalyst in the propulsion system for the attitude and altitude control of the satellite. The catalytic reaction for propulsion is a simple decomposition of hydrazine as shown in the following equation.



Hydrazine decomposition is a highly exothermic reaction to elevate the temperature to 1273 K [1,2]. Therefore, the catalyst should be durable at such high temperature. Further, the hydrazine decomposition generated a large pressure gradient inside the catalyst pellet because of the conversion of liquid hydrazine to gaseous species such as hydrogen, nitrogen and ammonia. Often, several thousand pressure is achieved, resulting in the breakup of catalyst pellet and consequently wash-out of the catalyst from the thruster [2]. Thus, the catalyst should maintain its decomposition activity at high pressure and high temperature condition with the incorporated noble concept and design for mass transfer and heat dissipation. In fact, no catalytic material seems to be durable under

such harsh reaction environment otherwise the suitable structural modification is made. There are two types of commercial catalysts, S-405 and HKC-12GA for hydrazine decomposition [3].

There were distinct morphological characteristics of the S-405 catalyst in which the well defined crystal morphologies were observed and the cubic to hexagonal crystal stuck together to form larger crystal aggregates [4–6]. Also, there are a large number of holes at the surface of the catalyst that can be advantageous for facile diffusion of reactant and product gas. While, there is no such well shaped crystal in KC-12GA catalyst [1]. Further, the surface of the catalyst showed less number of holes for diffusion of reactant and product gas. Fig. 1 shows the morphologies of both catalysts in the SEM micrograph. Still the structural and morphological similarities were shared in both catalysts. The catalysts were supported on a priority alumina that had many holes at the alumina. However, there is limited information on the alumina support though the related patents were disclosed, thus promoting the investigation of alumina support and the catalyst preparation technology.

As hydrazine decomposition reaction proceeds, there were large pressure and temperature gradients inside the catalyst pellet [2]. Thereby, the mechanical stability of the catalyst pellet was very important. The other way to relieve the pressure and temperature gradient can be providing the pathway for the mass and heat transfer. This can be accomplished with the incorporation of various pore sizes from macro to meso even micropore into the alumina using suitable structural modification.

In the present work, the large crystalline aluminium hydroxide of ca. 50 μm was transformed into rehydratable alumina [7,8]

\* Corresponding author. Tel.: +82 62 530 1902.

\*\* Co-corresponding author.

E-mail addresses: [skim@kari.re.kr](mailto:skim@kari.re.kr) (S.K. Kim), [sjcho@chonnam.ac.kr](mailto:sjcho@chonnam.ac.kr) (S.J. Cho).

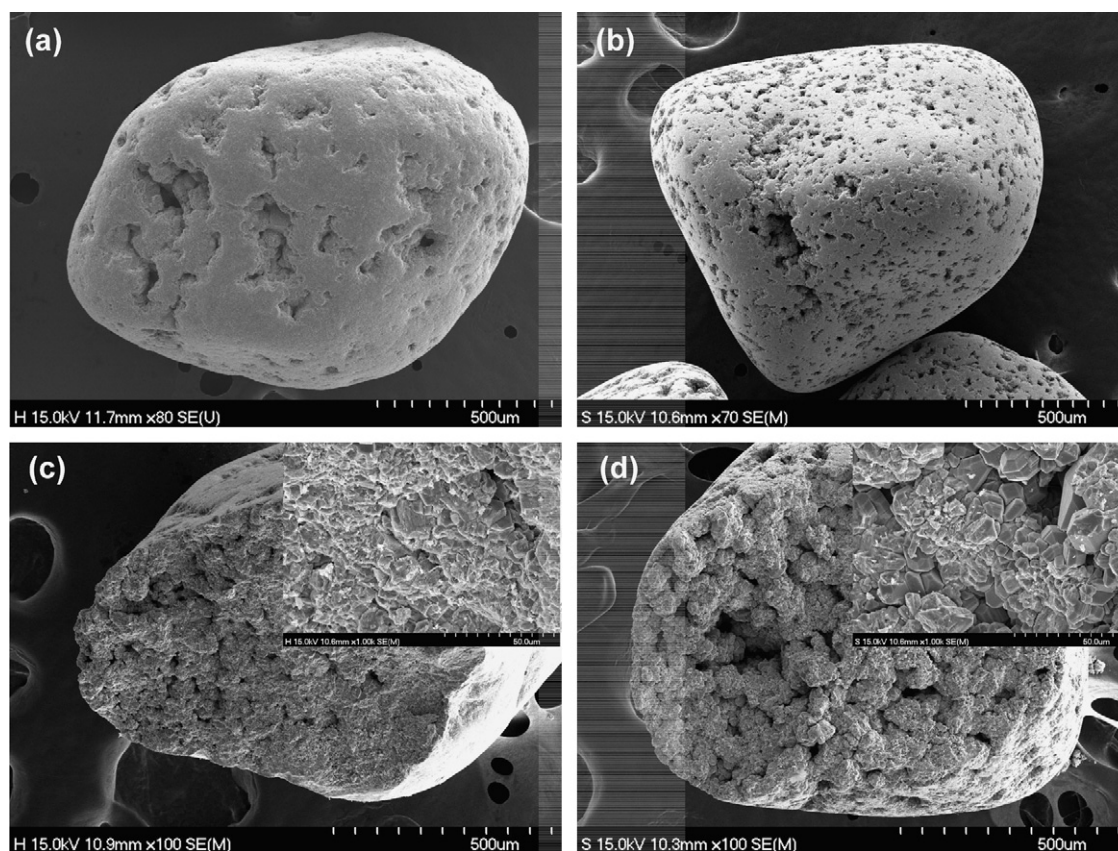


Fig. 1. (a and c) Scanning electron micrograph of the KC-12GA and (b and d) Shell-405.

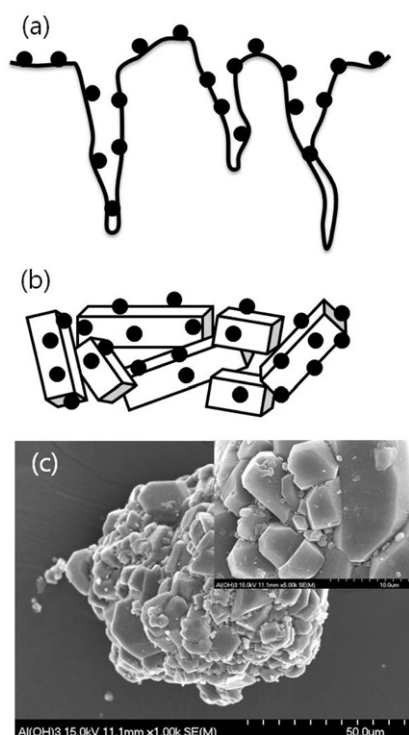


Fig. 2. Schematic feature of (a) amorphous alumina support and (b) crystalline alumina support. The dark circle indicates the Ir nanoparticle. The micrograph of the polycrystalline  $\text{Al}(\text{OH})_3$  was shown in (c).

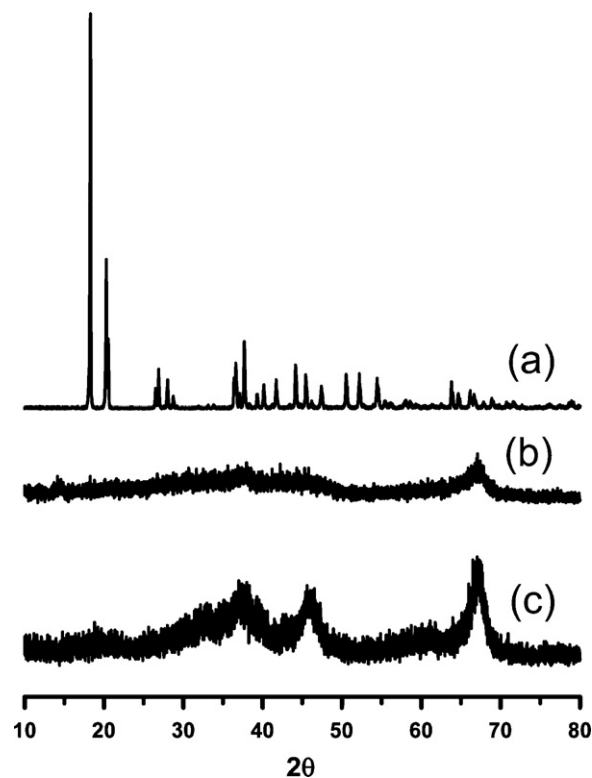


Fig. 3. XRD patterns of (a)  $\text{Al}(\text{OH})_3$ , gibbsite, (b) dehydrated alumina powder and (c) the support granule.

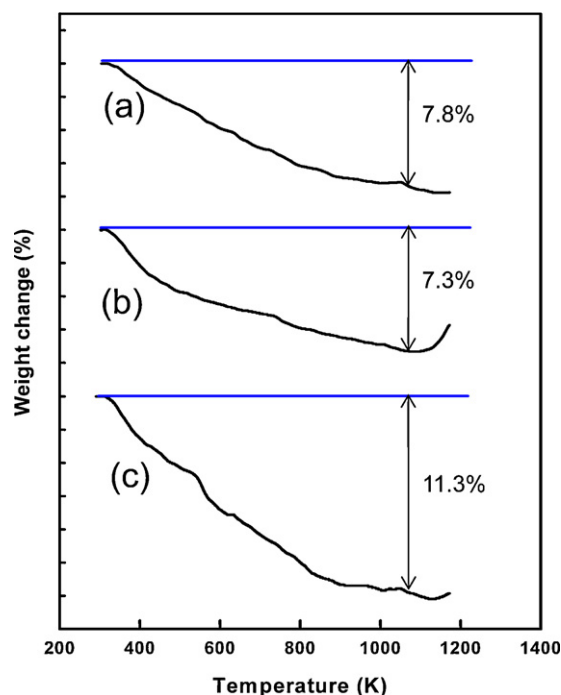


Fig. 4. TGA pattern of the dehydrated alumina powder at (a) 750 K, (b) 800 K and (c) 850 K.

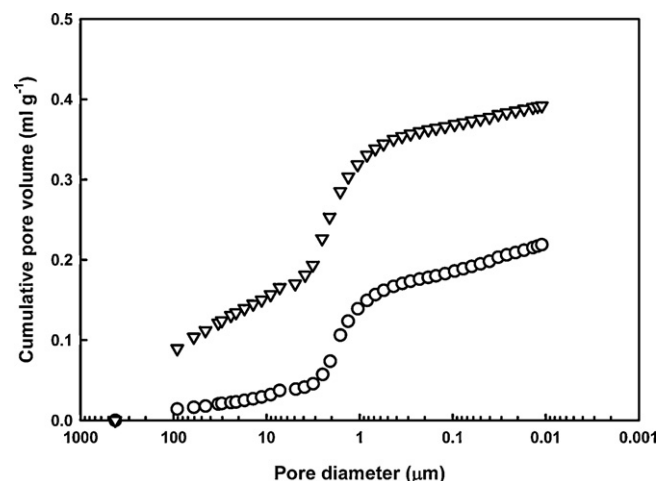


Fig. 6. Effect of the micro sized filler: (▽) with and (○) without the filler.

and subsequently was fabricated into granule for the metal catalyst preparation. The catalyst has been characterized with X-ray diffraction, mercury intrusion and extrusion method, hydrogen chemisorption, scanning electron micrographs and transmission electron micrograph. The activity of hydrazine decomposition was measured using dual thruster module until end of life.

## 2. Experimental

$\text{Al}(\text{OH})_3$  (KC Chemical Corp.) was used as raw material for the preparation of the alumina powder through thermal pyrolysis for a few seconds at 800–1000 K. For such fast dehydration, aluminium trihydroxide was dropped into the tubular furnace. The length of the heating zone corresponded to less than 5 s heating in the range of 800–1000 K. The alumina pellet was extruded from those 50  $\mu\text{m}$  sized alumina powder, with a micron sized filler such as micro-crystalline cellulose, wood flour, etc. to introduce macro-mesopore structure. The severe attrition and high pressure extrusion more than 120 kg per  $\text{cm}^2$ , resulted in more uniform macropore. The crushing strength of the extruded pellets ranged from 10 to 15 N for the 14–18 mesh granule, sufficient for catalytic application.

Supporting Ir catalyst was performed using wet impregnation method with  $\text{IrCl}_3(\text{aq})$  solution. Multiple impregnation was necessary to obtain 30 wt%. During multiple impregnation, drying the sample up to 573–673 K converted Ir precursor into  $\text{IrO}_x$  phase [9,10]. Finally, the catalyst was reduced in flowing hydrogen at 673 K. The obtained catalyst was denoted as KCMC-7 (Korea Aerospace Research Institute-Chonnam National University Model Catalyst-7).

X-ray diffraction patterns were obtained using X-ray diffractometer equipped with Cu  $\text{K}\alpha$  and Ni-filter (D/MAX Ultima Rigaku) at 40 kV and 40 mA. Thermogravimetric analyses (TGA) were performed on an DSC-60, TGA-50H Thermal Analysis System

Table 1

Results for the Hg intrusion–extrusion measurements for the alumina sample.

Item	Value
Total intrusion volume ( $\text{mL/g}$ )	0.81
Total pore area ( $\text{m}^2 \text{g}^{-1}$ )	194
Average pore diameter (4 V/A, nm)	16.7
Bulk density ( $\text{g/mL}$ )	0.82
Apparent (skeletal) density ( $\text{g/mL}$ )	2.47
Porosity (%)	66.7
Threshold pressure (psi)	5.14
Permeability (mdarcy)	953.4
Tortuosity	5.93

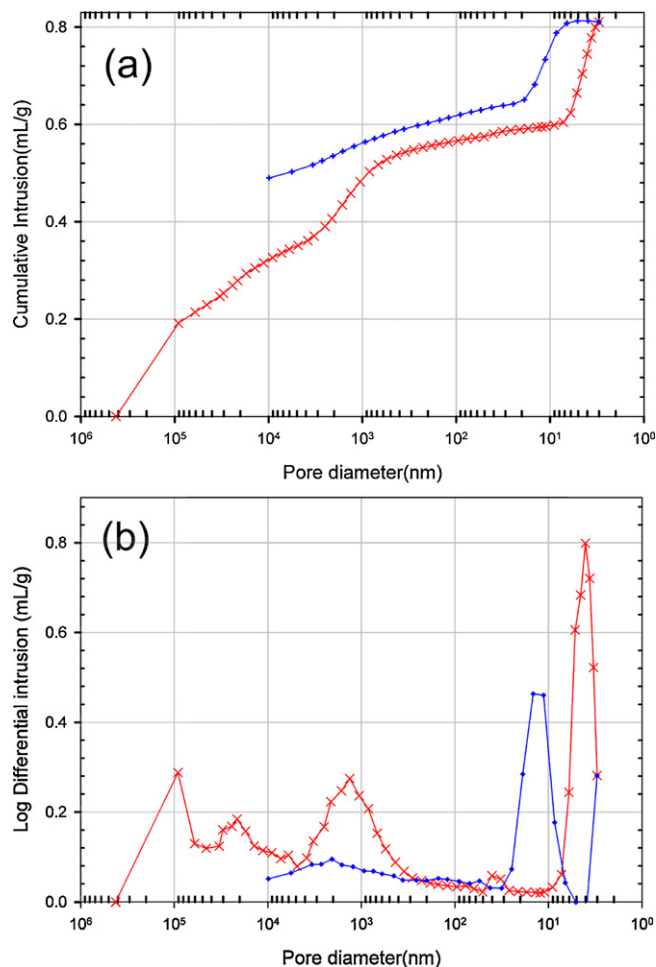
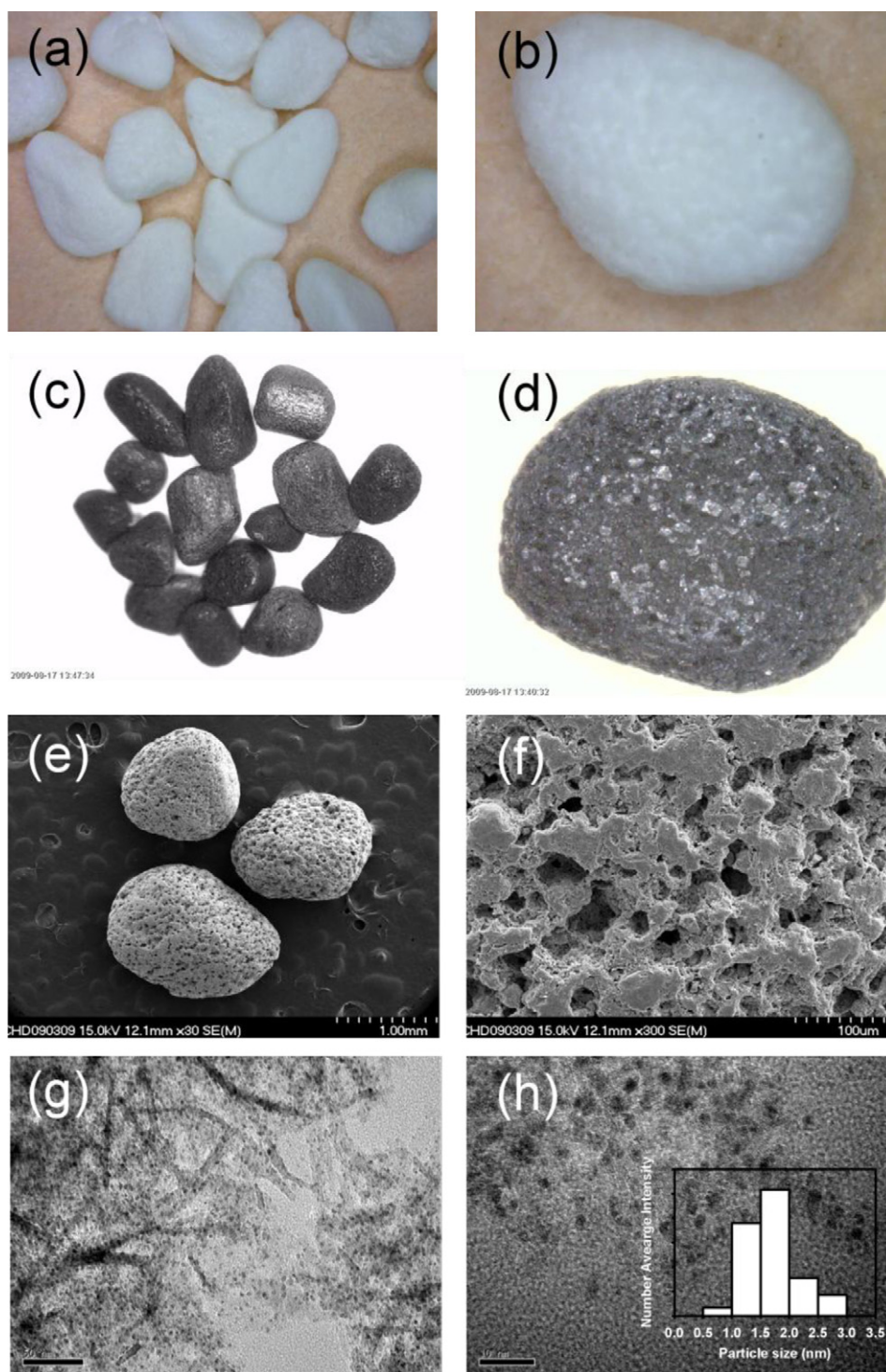


Fig. 5. (a) The cumulative pore volume and (b) its corresponding pore size distribution that was obtained from the mercury intrusion and extrusion measurements. The red and blue lines indicate the intrusion and extrusion, respectively.



**Fig. 7.** Micrographs of (a and b) alumina support granule, (c–f) Ir containing catalyst and (g and h) transmission electron micrograph of the Ir containing catalyst. The inset showed the particle size distribution obtained by measuring more than 100 particles.

(Shimadzu), where the weight losses related to the loss of water were further confirmed by differential analyses (DTA) using the same analyzer. Multinuclear MAS NMR measurements were performed mainly on a Varian UnityInova600 spectrometer at a spinning rate of 20 kHz. The cross-polarization  $^{27}\text{Al}$  MAS NMR spectra were measured at a  $^{27}\text{Al}$  frequency of 156.327 MHz with a  $\pi/8$  rad pulse length of 1.8  $\mu\text{s}$  and a recycle delay of 0.5 s. Approximately 600 pulse transients were accumulated, and the  $^{27}\text{Al}$  chemical shifts are reported relative to

an  $\text{Al}(\text{H}_2\text{O})_6^{3+}$  solution. Scanning electron micrographs (SEM) were obtained with EMAX instrument (Jeol S-4700). Also, the elemental analysis was performed using EDX attached to SEM. For transmission electron microscopy (TEM), the sample was dispersed in ethanol for 30 min using sonicator. The dispersion was drop onto the grid and dried repeatedly. The TEM micrograph was taken using Tecnai F20 at Korea Basic Science Institute Gwangju Branch.  $\text{N}_2$  BET adsorption–desorption isotherm was measured using ASAP2020 instrument (Micromeritics) after



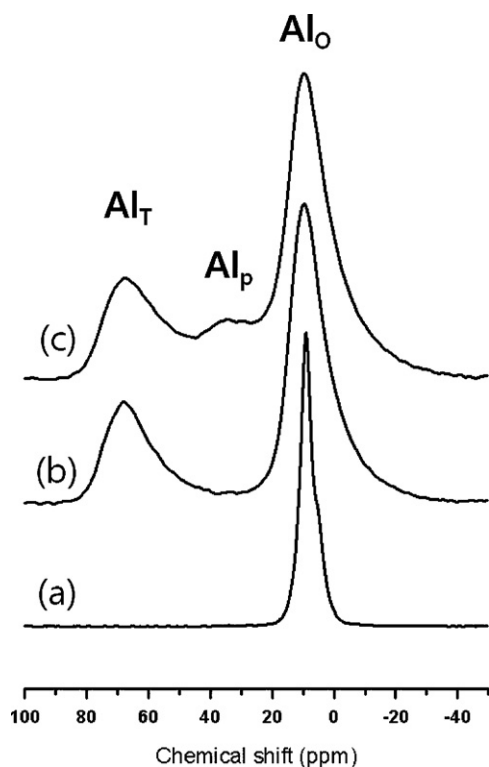


**Fig. 8.**  $^{27}\text{Al}$  MAS NMR spectra of (a)  $\text{Al}(\text{OH})_3$ , gibbsite, (b) dehydrated alumina powder and (c) the support granule.  $\text{Al}_\text{T}$ ,  $\text{Al}_\text{P}$  and  $\text{Al}_\text{O}$  were corresponded to tetrahedral, pentagonal and octahedral sites, respectively.

the sample was evacuated for 4 h at 573 K. For the hydrogen adsorption measurements at 298 K, a  $\sim 0.5$  g sample was placed in the adsorption cell equipped with a vertical stopcock. The cell was then evacuated to remove the adsorbed impurities at 573 K until  $1 \times 10^{-3}$  kPa. The adsorption isotherms of  $\text{H}_2$  were measured using a volumetric gas adsorption apparatus. The mercury intrusion and extrusion into the catalytic alumina was measured using AutoPore IV 9500 instrument (Micromeritics) at Korea Basic Science Institute Jeonju Branch.

The activity test of the catalyst was performed using 4.5 N class thruster similar to MRE-1 type produced from Northrop Grumman Corp. The sequence of the activity test was similar to the acceptance life test sequence reported in the literature [5].

### 3. Result and discussion

Mass and heat transfer are very important for hydrazine decomposition reaction since there was large pressure and temperature gradient inside the catalyst pellet when the hydrazine was decomposed into hot hydrogen, nitrogen and ammonia gases [2]. In general, most catalytically active sites are located deep inside amorphous alumina pore as Ir nanoparticle of which the size ranged from 1 to 2 nm. High temperature can cause either a sintering of metal particle inside the pore or a shrinkage of the pore, resulting in the pore blockage and consequently a loss of catalytic activity. On the other hand, it was possible that the liquid hydrazine filled the pore and subsequently was decomposed upon heating to create large pressure gradient to break up the catalyst granule. Hydrazine decomposition reaction generated large pressure increase inside the pore structure as shown in the case of Fig. 2(a). This phenomena can deteriorate the mechanical stability of the alumina particle resulting in external breakage of the catalyst pellet [2,3]. While, the alumina crystal may contain Ir nanoparticles at the surface without interpenetration into dense crystal inside shown in Fig. 2(b). Thus,

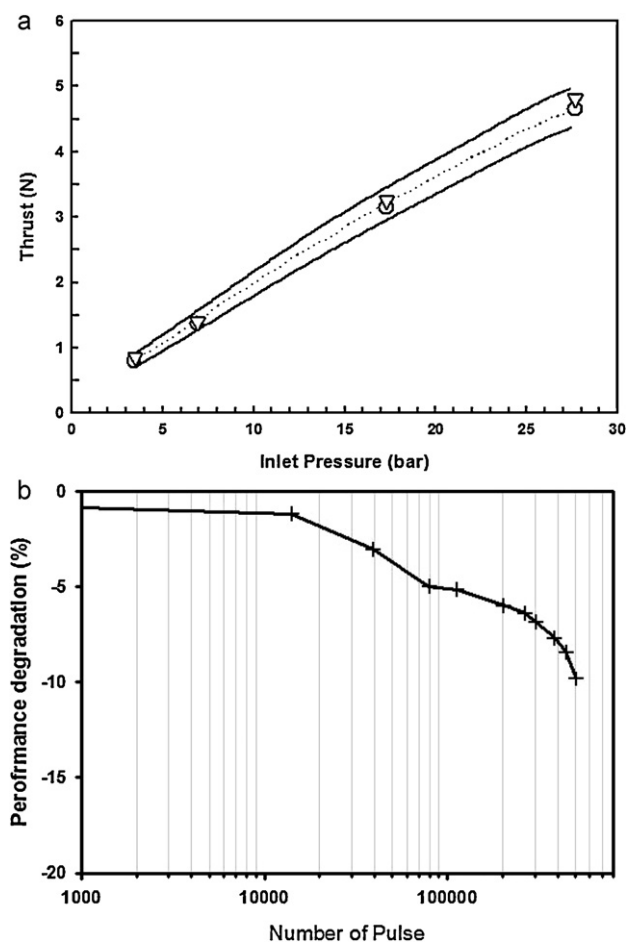


**Fig. 9.** (a) Thrust as a function of inlet pressure: after ( $\nabla$ ) 380,000 pulses and ( $\circ$ ) 550,000 pulses, respectively. (b) Performance degradation of the chamber pressure against the number of pulse. The inlet pressure was 24.1 bar under atmospheric condition.

the pressure can be relieved easily through three-dimensional network. This dissipation also accompanies heat, thereby increasing the thermal stability of the alumina support. Conceptually, it can be proposed that the pore structure of the alumina can be affected by the crystal size of alumina and the supporting metal nanoparticle on the corresponding surface can provide the close contact with the reactant, liquid hydrazine. Therefore, the topotatic transformation of aluminium hydroxide shown in Fig. 2(c) can allow the intercrystalline pore for facile mass and heat transfer.

The large polycrystalline aluminumtrihydroxide can be dehydrated at high temperature for the preparation of catalyst granule. It was reported that the aluminumtrihydroxide can be transformed into  $\rho\text{-Al}_2\text{O}_3$  upon fast dehydration at 800–1000 K [7,8]. The  $\rho\text{-Al}_2\text{O}_3$  is rehydratable and also bondable alumina when a suitable amount of water was added. Thus it was possible to fabricate the obtained  $\rho\text{-Al}_2\text{O}_3$  into the tubular shape which was crushed and subsequently smoothed. Fig. 3 shows the XRD patterns of the alumina sample. The aluminium trioxide was found to contain gibbsite structure. The gibbsite structure was disappeared upon fast dehydration and the typical  $\rho\text{-Al}_2\text{O}_3$  structure was formed, which was in good agreement with that reported [11]. Further, the fabrication of  $\rho\text{-Al}_2\text{O}_3$  powder with the micron sized filler, 300 mesh wood flour, led to the formation of  $\gamma\text{-Al}_2\text{O}_3$  structure. The loss of water measured by TGA as shown in Fig. 4 was 7–11 wt% for the dehydrated to  $\rho\text{-Al}_2\text{O}_3$  powder, corresponding to the structure of  $\text{Al}_2\text{O}_3 \cdot \text{H}_2\text{O}$ . It was reported that the typical water content in the  $\rho\text{-Al}_2\text{O}_3$  was 4–11 wt% [7–10]. Therefore, the fast dehydration and subsequent

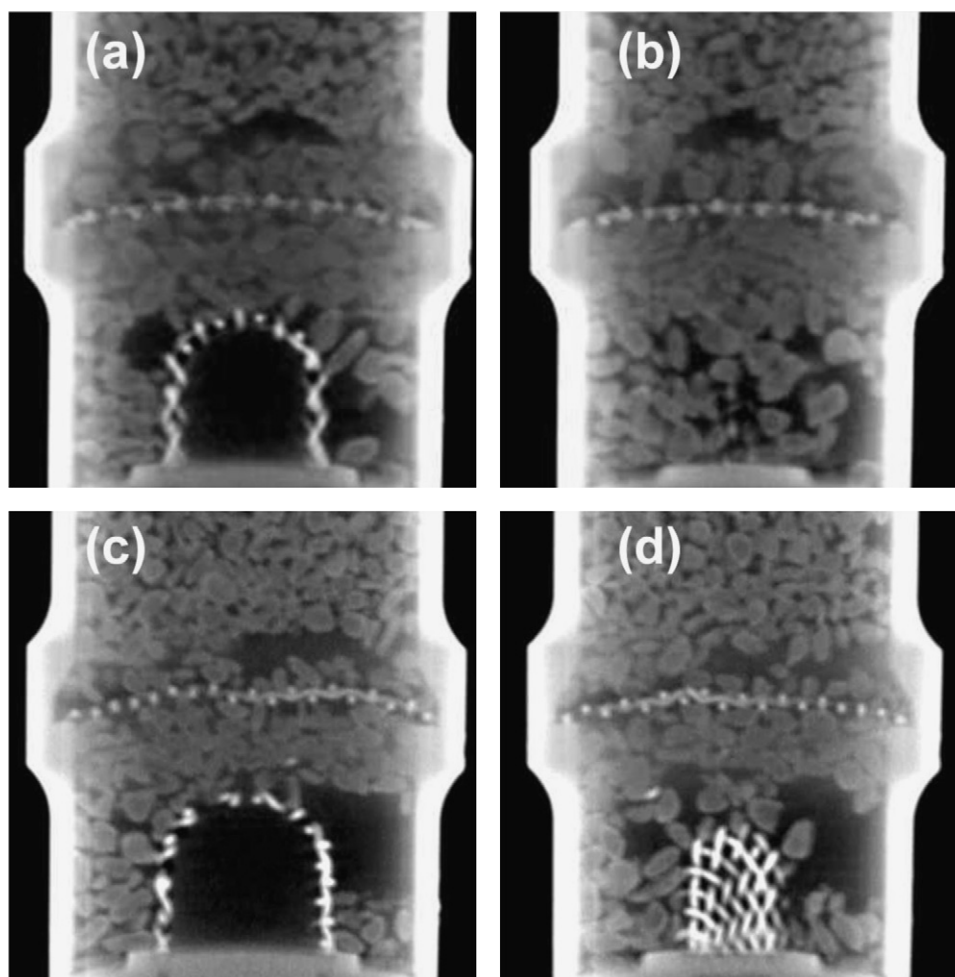


**Fig. 10.** Computed tomography of the upper catalyst bed of the 4.5 N class thruster: (a and b) after 77,000 pulses and (c and d) 550,000 pulses, respectively.

fabrication of the catalyst granule accompanied with the structural change, gibbsite to  $\rho$ - $\text{Al}_2\text{O}_3$  and finally  $\gamma$ - $\text{Al}_2\text{O}_3$ .

Fig. 5 and Table 1 show the results of mercury intrusion and extrusion experiment on the obtained alumina support. The mercury intrusion was increased with increasing pressure corresponding to the small pore size. The mercury intrusion and extrusion shows the hysteresis due to the pore shape. The pore size distribution from the intrusion and extrusion was also shown in Fig. 5. Starting from the large pore diameter corresponding to macro pore, the mesopore size about 3–4 nm was observed. There was continuous distribution of the pore size from 100  $\mu\text{m}$  to 3 nm. The result of  $\text{N}_2$  adsorption and desorption at 77 K as listed in Table 2 also showed the material contained meso porous structure. The maximum permeability of the alumina support was ca. 1000 mdarcies, corresponding to the threshold pressure around 5 psi as shown in Table 1. The permeability of the alumina support can be controlled to 100–300 mdarcies. Thus, such an high permeability originated from the porous network of macro, meso and micro pores provides the pathway for facile mass and heat

transfer [2]. Especially, the macropore was generated when the micron sized filler, 20  $\mu\text{m}$  was incorporated as shown in Fig. 6. Without the filler, the fraction corresponding to the macropore was decreased drastically. Thus, the use of the filler was essential for the formation of macropore.

Fig. 7 shows the micrographs of the smoothed alumina support and the corresponding catalyst. As shown in Fig. 7, there were many micron sized hole to facilitate mass and heat transfer. The size of iridium particle was around 2 nm. The hydrogen chemisorption also suggested 1.5–2.0 nm particle size roughly even for high loading, 30 wt% [9,10]. Table 2 also compares the surface characteristics of the catalyst with the commercially available catalyst [3]. The amount of the hydrogen chemisorption on the present catalyst was much higher than those of the commercial catalyst by 30%. It was speculated that the pentagonal Al site as shown in Fig. 8 was abundant after the fabrication of the catalyst granule. Such pentagonal Al site rather than tetrahedral Al site was reported to be anchoring site for the formation of small metal particle in which the loaded metal atom was attached to the coordinatively unsaturated pentagonal preferentially [12]. Thus, high amount of the pentagonal Al site can contribute the formation of small Ir nanoparticle at such a high loading.

Fig. 9 shows the result of the activity test of the catalyst using 4.5 N class thruster similar to MRE-1 type. The sequence of the activity test was consisted of the continuous and pulse mode injection of hydrazine. The total number of pulse for flight model test was around 77,000 and the amount of hydrazine consumed was ca. 25 kg [4]. Before the activity test, the thrust was measured as a

**Table 2**  
Results for the surface characterization of the hydrazine decomposition catalyst.

Item	Shell405	KC12GA	KCMC-7
BET ( $\text{m}^2 \text{g}^{-1}$ )	111	149	125
Pore volume ( $\text{cm}^3 \text{g}^{-1}$ )	0.14	0.13	0.18
$\text{H}_2$ chemisorption ( $\mu\text{mol g}^{-1}$ )	347	408	461
Ir (wt%)	30.7	30.8	33.0

function of inlet pressure from 50 psi to 350 psi. The thrust should be near nominal line with  $\pm 12\%$  error. After 500,000 pulses, the thrust was still within the range of the limit allowed though the activity deterioration increased to 10%. Therefore, the macro-mesopore structured alumina catalyst showed the high potential for the hydrazine decomposition reaction under harsh condition, high pressure and high temperature.

The deactivation of catalytic activity in the thruster is known to be occurred because of the generation of voids in the catalyst bed, consequently loss of the active surface [3]. These voids can be formed during the acceptance test and launch vibration and also with the breakup of catalyst grains. The computed tomography (CT) of the upper catalyst bed in the thruster was taken to show the fraction of void. Fig. 10 shows the CT of the thruster after 77,000 pulses and 550,000 pulses, respectively. The catalyst grains were packed well after the screen mesh even after the large number of pulses. However, the catalyst packing near the injector with round screen mesh was not good. Such void fraction in the catalyst bed was increased with the number of pulses, which decreased the catalytic performance, that is, the decrease of thrust. Thus, the mechanical stability of the catalyst grains is very important to improve the catalytic performance of the hydrazine decomposition reaction. In this respect, the breakup or attrition of the catalyst grains seems to be the major pathway for the performance degradation.

#### 4. Conclusion

The macro-mesopore structure alumina catalyst was developed for the hydrazine decomposition reaction for the attitude and altitude control of the satellite. The topotactically transformed alumina catalyst contained higher permeability to allow the facile mass and heat transfer, thereby maintaining the hydrazine decomposition activity under the reaction condition. The use of the filler in the fabrication of the catalyst granule generated the macropore around

20  $\mu\text{m}$ . The alumina support containing macro and mesopore network and high amount of coordinatively unsaturated pentagonal Al sites can be applied in various catalytic processes, which was especially suitable for the high pressure or temperature and diffusion limited reaction.

#### Acknowledgements

This work was supported by Korea Aerospace Research Institute. SJ thanks Pohang Accelerator Laboratory for the generous permission to use the XAFS facility at BL-3C1.

#### References

- [1] W.E. Armstrong, L.B. Ryland, H.H. Voge, Catalyst comprising Ir and Ru for hydrazine decomposition, U.S. Patent 4,124,538.
- [2] C. Kappenstein, J.P. Joulin, *Advances in Science and Technology* 45 (2006) 2143.
- [3] W.F. Taylor, W.T. Webber, External Catalyst Breakup Phenomena, Exxon Research and Engineering Co. Government Research Laboratory, Linden, NJ, 1975.
- [4] D. Goto, H. Kagawa, A. Hattori, K. Kajiwaru, F. Ueno, J. Umeda, S. Iihara, Proceedings of the 3rd European Workshop on Hydrazine, Calvi, Sardinia, Italy, 9 June 2004, 2004.
- [5] M. Patrick, P. Chris, P. Charles, T. Alicia, U. Walter, J.W. Michael, Confidence testing of Shell-405 and S-405 catalysts in a monopropellant hydrazine thruster, in: Proceedings of the 41st AIAA/ASME/SAE/ASEE Joint Propulsion Conference & Exhibit, Tucson, AZ, 2005, p. 3952.
- [6] E.J. Wucherer, T. Cook, M. Stiefel, R. Humphries, J. Parker, Hydrazine catalyst production-sustaining S-405 technology, in: Proceedings of the 39th AIAA/ASME/SAE/ASEE Joint Propulsion Conference and Exhibit, Huntsville, AL, 2003, p. 5039.
- [7] S.D. Vaidya, N.V. Thakkar, *Mater. Lett.* 51 (2001) 295.
- [8] S.D. Vaidya, N.V. Thakkar, *J. Phys. Chem. Solids* 62 (2001) 977.
- [9] Y.B. Jang, T.H. Kim, M.H. Sun, J. Lee, S.J. Cho, *Catal. Today* 146 (2009) 196.
- [10] S.J. Cho, J. Lee, Y.S. Lee, D.P. Kim, *Catal. Lett.* 109 (2006) 181.
- [11] C.S. John, N.C.M. Alma, G.R. Hays, *Appl. Catal.* 6 (1983) 341.
- [12] J.H. Kwak, J.Z. Hu, D. Mei, C.W. Yi, D.H. Kim, C.H.F. Peden, L.F. Allard, J. Szanyi, *Science* 325 (2009) 1670.